DOI: 10.1002/ange.200901175

Fluorescent Probes

A Two-Photon Tracer for Glucose Uptake**

Yu Shun Tian, Hyang Yeon Lee, Chang Su Lim, Jongmin Park, Hwan Myung Kim, Yoo Na Shin, Eun Sun Kim, Hoon Jae Jeon, Seung Bum Park, and Bong Rae Cho**

Glucose is the principal energy source essential for cell growth. Fast-growing cancer cells exhibit a high rate of glycolysis; hence, the rate of glucose uptake is faster in these cells, primarily due to overexpression or enhanced intracellular translocation of glucose transporters (GLUTs) and increased activity of mitochondria-bound hexokinases in the tumor.[1] To monitor glucose metabolism in living systems, a variety of tracers, such as [^{18}F]-2-fluoro-2-deoxyglucose (^{18}FDG), 2-[*N*-(7-nitrobenz-2-oxa-1,3-diazol-4-yl)-amino]-2-deoxy-D-glucose (2-NBDG; Scheme 1), and IR dye 800CW-2DG, have been developed. ^{18}FDG is widely used in the in vivo analysis of glucose metabolism by positron emission tomography (PET),[2–4] whereas 2-NBDG and IR dye 800CW-2DG are fluorescent probes that have been used for studying cellular metabolic functions involving GLUTs and in tumor-imaging studies.[5–8] Recently, we developed a new fluorescent probe, cyanine-3-linked *O*-1-glycosylated glucose (Cy3-Glc-α; Scheme 1), which is a better glucose probe than 2-NBDG because it can be used without glucose starvation, produces a much brighter image, and can be applied for the screening of anticancer agents.[9]

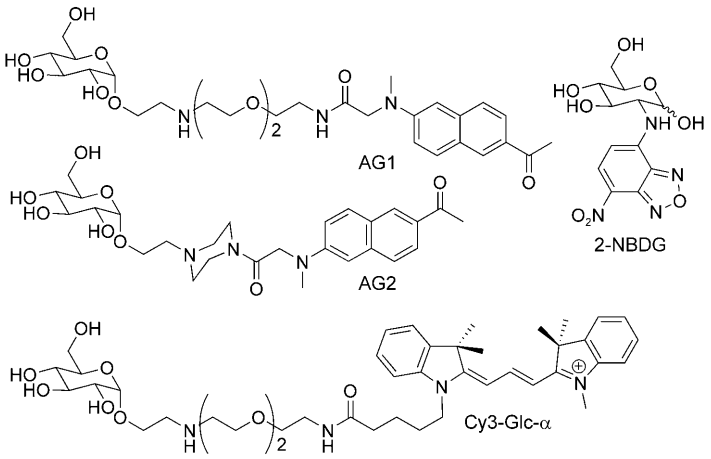

Scheme 1. Structures of fluorescent tracers AG1, AG2, 2-NBDG, and Cy3-Gly-α.

In one-photon microscopy (OPM), the probes are excited with short-wavelength light (≈350–550 nm); this, however, limits their application in tissue imaging, owing to inherent problems such as shallow penetration depth (<80 μm), interference by cellular autofluorescence, photobleaching, and photodamage.[10,11] To overcome these problems, it is crucial to use two-photon microscopy (TPM), which utilizes two near-infrared photons for excitation. TPM offers a number of advantages over OPM, including greater penetration depth (>500 μm), localized excitation, and longer observation times.[12,13] In particular, the extra penetration depth afforded by TPM is an essential element for application in tissue-imaging studies because the artifacts arising from surface preparation, such as damaged cells, can extend over 70 μm into the tissue interior.[14] However, visualization of glucose uptake by live cells and tissues with two-photon (TP) tracers has not been reported so far.

The requirements for a TP tracer to visualize glucose uptake include sufficient water solubility for staining cells and tissues, preferential uptake by cancer cells, a large TP cross-section for a bright TPM image, pH resistance, and high photostability. Our strategy was to link α-D-glucose with the fluorophore 2-acetyl-6-dimethylaminonaphthalene (acedan) through 3,6-dioxaoctane-1,8-diamine or a piperazine linkage (in AG1 and AG2, respectively; Scheme 1), so that the tracers are transported into the cells through the glucose-specific mechanism. Acedan is a polarity-sensitive fluorophore that has been successfully employed in the development of TP probes for the cell membrane,[15] metal ions,[16–18] and acidic vesicles.[19] We now report that these tracers facilitate the visualization of glucose uptake in cancer cells and live tissues at a depth of 75–150 μm for more than 3000 s and can be used for screening anticancer agents.

The preparation of AG1 and AG2 is shown in Scheme 2. 6-Acetyl-2-[*N*-methyl-*N*-(carboxymethyl)amino]naphthalene

[*] H. Y. Lee, J. Park, Prof. Dr. S. B. Park
Department of Chemistry, Seoul National University
Seoul 151-747 (Korea)
Fax: (+82) 2-884-4025
E-mail: sbpark@snu.ac.kr
Dr. Y. S. Tian, C. S. Lim, Y. N. Shin, Prof. Dr. B. R. Cho
Department of Chemistry, Korea University
1-Anamdong, Seoul 136-701 (Korea)
Fax: (+82) 2-3290-3544
E-mail: chobr@korea.ac.kr
Prof. Dr. H. M. Kim
Department of Chemistry, Ajou University (Korea)
Dr. E. S. Kim, Prof. Dr. H. J. Jeon
School of Medicine, Korea University

[**] This work was partly supported by a Korea Science and Engineering Foundation (KOSEF) grant funded by the Korea Ministry of Education, Science, and Technology (MESF) (grant no.: R0A-2007-000-20027-0), the WCU program through the KOSEF funded by the MESF, and the MarineBio Technology Program funded by the Ministry of Land, Transport, and Maritime Affairs (MLTM), Korea. H.Y.L. and J.P. received BK21 Scholarships and Seoul Science Fellowships.

Supporting information for this article is available on the WWW under http://dx.doi.org/10.1002/anie.200901175.

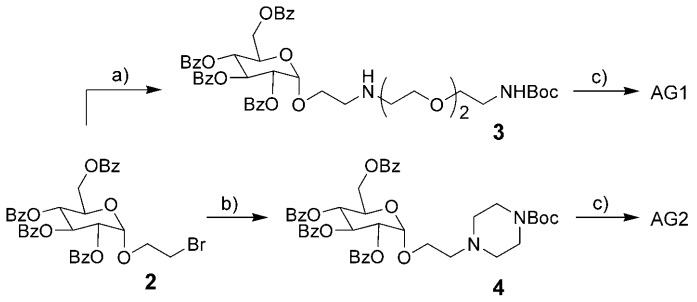

Scheme 2. a) *N*-Boc-3,6-dioxaoctane-1,8-diamine, Et_3N, DMF, 50 °C; b) *N*-Boc-piperazine, Et_3N, DMF, 50 °C; c) 1. NaOMe, MeOH; 2. 50% TFA/CH_2Cl_2; 3. **1**, EDC, DIPEA, DMF. Boc: *tert*-butoxycarbonyl; DMF: *N*,*N*-dimethylformamide; TFA: trifluoracetic acid; EDC: 3-(3-dimethylaminopropyl)-1-ethylcarbodiimide; DIPEA: *N*,*N*-diisopropylethylamine.

(**1**), **2**, and **3** were prepared by the method used in our previous studies.[4,15–19] The reaction of **2** with *N*-Boc-piperazine afforded **4** in 70% yield. AG1 and AG2 were prepared in 26 and 86% yields, respectively, by treating **3** and **4** with **1** (see the Supporting Information).

The fluorescence spectra of AG1 and AG2 showed gradual bathochromic shifts with increases in the solvent polarity (E_T^N) with the following order of solvents: 1,4-dioxane < DMF < EtOH < H_2O (Figure S1 and Table S1 in the Supporting Information). The large bathochromic shifts upon increases in the solvent polarity indicate the utility of these molecules as polarity probes. Both compounds show strong fluorescence in all of the solvents. Moreover, they are pH insensitive in the biologically relevant pH range (Figure S1c and S1f in the Supporting Information). The TP action spectrum of AG1 determined by the two-photon-excited fluorescence (TPEF) method[20] indicated a $\Phi\delta$ value of $\approx$90 GM at 780 nm, which is much larger than those observed for Cy3-Glc-α and 2-NBDG (Figure 1 and Table 1). Hence, the TPM images of the samples stained with AG1 or AG2 would appear much brighter than those stained with Cy3-Glc-α or 2-NBDG.

The optimum concentration of these probes for the cellular uptake experiments was determined by comparing the TPM images of A549 cells treated with 6, 12.5, 25, 50, and 100 μM of AG1 and AG2 for 30 min. The TPM images appeared brighter as the probe concentration was increased up to 50 μM; however, at 100 μM concentrations, some cell death was observed (Figure S2 in the Supporting Information). Moreover, a higher uptake rate and a brighter TPM image were obtained when the cells were treated with AG2 than when they were treated with AG1 (see Figure 3A and Figure S3 in the Supporting Information). Furthermore, the effect of AG2 on the viability of cells was studied by using the CCK-8 kit: AG2 showed negligible toxicity, which indicates that it could be applied for live-cell imaging (Figure S4 in the Supporting Information). Therefore, we used 50 μM AG2 as the optimum concentration in further cellular uptake experiments.

The pseudocolored TPM images of cultured A549 cells treated with 50 μM AG2 showed intense spots and homogeneous domains with two-photon emission maxima at 461 (marked in blue in Figure 2A and B) and 497 nm (marked in red), respectively. The TPEF spectrum of the intense spots was asymmetrical and could be fitted to two Gaussian functions with emission maxima at 445 (green line in Figure 2B) and 488 nm (orange line), whereas the TPEF spectrum of the homogeneous domain could be fitted to a single Gaussian function (pink line) with an emission maximum at 497 nm. The longer wavelength band of the dissected Gaussian function (orange line in Figure 2B) is similar to the band of the single Gaussian function (pink line). This result suggests that the probe is located in two regions of different polarity: a more polar one that is likely to be cytosol and a less polar one that is likely to be membrane associated. Moreover, the shorter wavelength band (green in Figure 2B) in the dissected Gaussian functions decreases to the baseline at wavelengths of less than 520 nm. Consistently, the TPM image collected at 520–620 nm is homogeneous without

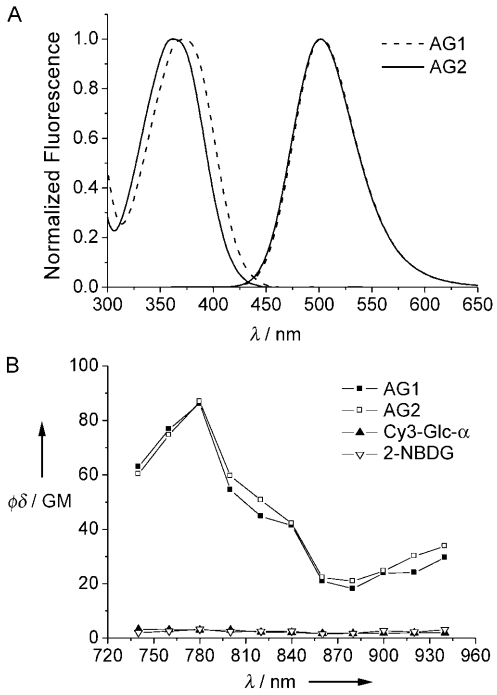

Figure 1. A) One-photon absorption and emission spectra of AG1 and AG2 in phosphate-buffered saline (PBS) buffer (137 mM NaCl, 3 mM KCl, 10 mM Na_2HPO_4, 2 mM KH_2PO_4, pH 7.4). B) Two-photon action spectra for AG1, AG2, Cy3-Glc-α, and 2-NBDG in PBS buffer.

Table 1: Photophysical data for AG1, AG2, Cy3-Glc-α, and 2-NBDG.[a]

Compound	$\lambda_{max}^{(1)}/\lambda_{max}^{(fl)}$ [b]	Φ[c]	$\lambda_{max}^{(2)}$ [d]	δ_{max} [e]	$\Phi\delta_{max}$ [f]
AG1	373/501	0.90	780	95	86
AG2	375/501	0.56	780	155	88
Cy3-Glc-α	545/555	0.01	n.d.[g]	n.d.[g,h]	n.d.[g,h]
2-NBDG	465/540[i]	n.d.[g]	n.d.[g]	n.d.[g,h]	n.d.[g,h]

[a] All measurements were performed in PBS buffer. [b] λ_{max} values of the one-photon absorption and emission spectra in nm. [c] Fluorescence quantum yield, ±15%. [d] λ_{max} value of the two-photon absorption spectrum in nm. [e] The peak two-photon action cross-section in 10^{-50} cm^4/photon (GM), ±15%. [f] Two-photon action cross-section in GM. [g] n.d.: not determined. [h] The two-photon-excited fluorescence intensity was too weak to allow accurate measurement of the cross-section. [i] Reference [25].

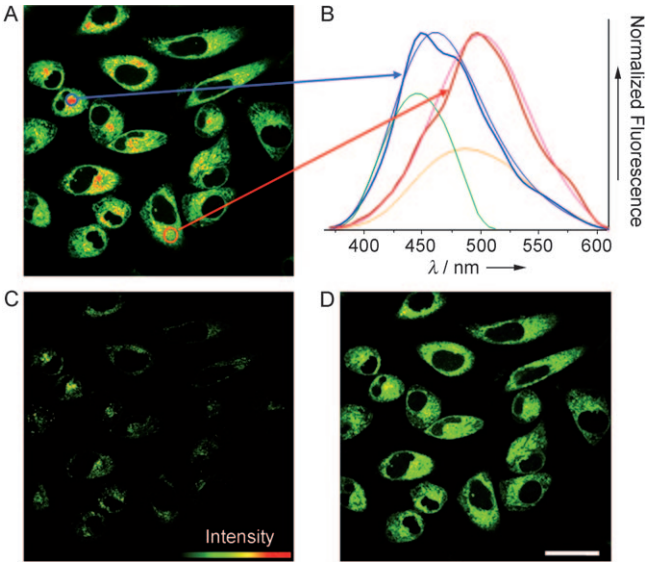

Figure 2. Pseudocolored TPM images of A549 cells incubated with 50 μM AG2 for 10 min, collected at A) 360–620, C) 360–460, and D) 520–620 nm. B) Two-photon-excited fluorescence spectra from the hydrophobic (marked in blue) and hydrophilic (marked in red) regions of the AG2-labeled A549 cells. The thin pale blue and pink curves represent the dissected Gaussian functions for the blue and red bands, respectively. The orange and green lines are discussed in the text. The excitation wavelength was 780 nm. The images shown are representative of the images obtained in the repeat experiments ($n = 5$). Scale bar: 30 μm.

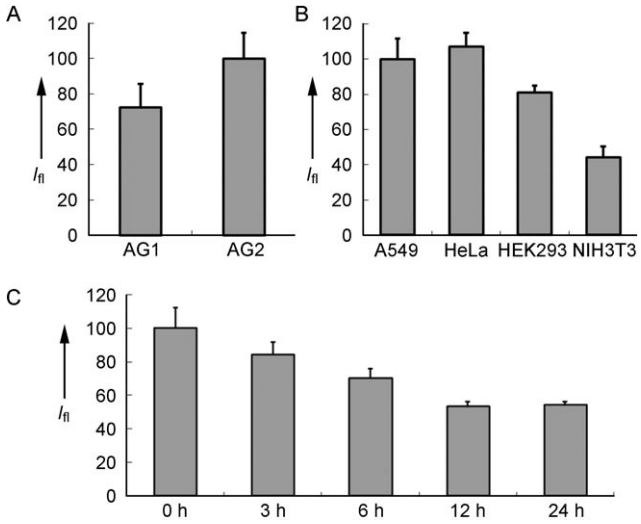

Figure 3. A) Relative AG1 and AG2 uptake by A549 cells. B) Relative AG2 uptake in cancer cells (A549, HeLa) and normal cells (HEK293, NIH/3T3). C) Relative AG2 uptake by A549 cells after treatment with taxol (9.8 μM) for 0, 3, 6, 12, and 24 h. Cells were incubated with AG1 or AG2 (50 μM) for 10 min, either before (A and B) or after (C) treating the cells with taxol (9.8 μM) for the designated period of time, and TPEF intensities from 40–60 cells were determined by photomultiplier tube. The data are the average of at least five independent experiments.

intense spots (Figure 2D), whereas the one collected at 360–460 nm clearly shows them (Figure 2C). Similar results were reported for acedan-derived TP probes for Mg^{2+} (AMg1)[16] and Ca^{2+} ions (ACa1).[17] Therefore, cytosolic AG2 can be selectively detected by using the detection window of 520–620 nm, with minimal interference from the membrane-bound probes. Furthermore, the TPM images of A549 cells costained with AG2 and MitoTracker, a well-known one-photon fluorescent (OPF) probe for mitochondria,[21] merged well with the OPM image (Figure S5 in the Supporting Information), which indicates that the probes are predominantly located in the mitochondria.

To assess whether AG2 is selectively taken up by cancer cells, the efficiencies of AG2 uptake by A549 (lung carcinoma cell line), HeLa (cervical cancer cell line), HEK293 (human embryonic kidney 293 cell line), and NIH/3T3 (murine fibroblast cell line) cells were compared. AG2 uptake was most efficient in A549 and HeLa cells, followed by HEK293 and NIH/3T3 cells (Figure 3B and Figure S7A in the Supporting Information); this result is similar to that obtained in the case of Cy3-Glc-α[9] and confirms the selective uptake of AG2 by cancer cells with enhanced glucose metabolism. The cellular uptake experiment showed that AG2 effectively competes with D-glucose in the media for cellular uptake; the fluorescence intensities of AG2 in A549 cells inoculated with media containing 10 mM or 50 mM D-glucose were reduced by about 16 and 74%, respectively, as compared to that with glucose-depleted medium, and the fluorescence intensity was not affected by medium containing L-glucose (50 mM; Figure S6 in the Supporting Information). Furthermore, AG2 uptake was not influenced by the presence of 55 mM D,L-alanine, which indicates that osmotic pressure does not have an impact on AG2 uptake. These results suggest that AG2 is a glucose analogue that is taken up by the cells through a glucose-specific transport system and not by passive diffusion.[1,9,22,23] Therefore, AG2 can be used for visualizing glucose uptake in living cells by TPM, without subjecting the cells to glucose starvation.

To demonstrate the utility of this probe, we investigated the effects of taxol on AG2 uptake by A549 cells. It was expected that the anticancer agent would depress the cellular metabolism and thereby reduce glucose uptake in the cancer cells.[9] The cells were incubated with the anticancer agent for 1, 3, 6, 12, and 24 h, washed with PBS, treated with AG2, and then imaged. The cellular uptake of AG2 was lower with longer incubation times (Figure 3C and Figure S7B in the Supporting Information). Dose-dependent uptake of AG2 was also observed with taxol concentrations of 49 nM, 490 nM, and 9.8 μM (Table 2). Another anticancer agent, combretastatin, also inhibited AG2 uptake in a similar manner (Table 2). Hence, AG2 can be used for screening anticancer agents in live cells by TPM.

Table 2: Dose dependence of AG2 uptake by A549 cells in the presence of various concentrations of anticancer agents.

	AG2 uptake [%]	
	after 6 h	after 12 h
taxol (9.8 μM)	69.5	50.7
taxol (490 nM)	89.6	69.5
taxol (49 nM)	97.6	81.8
combretastatin (2 μM)	70.2	53.2

We further assessed the utility of AG2 in tissue imaging for the diagnosis of colon cancer, for which we used images of normal- and cancer-tissue slices from colon-cancer patients. The bright-field image of the normal tissue clearly revealed the presence of glands on the tissue surface. However, the cancer tissue appeared almost amorphous and did not have a definite structure (Figure 4A and Figure S8A in the Supporting Information). The tissues were incubated in artificial cerebrospinal fluid (ACSF) for 4 h at 37 °C in the absence and presence of taxol (50 μM), after which the AG2 uptake was monitored by TPM by following the change in TPEF at a depth of 100 μm. The result shows that AG2 uptake in the cancer tissue is much faster than that in the normal tissue and that the cancer tissue pretreated with taxol for 4 h exhibits much slower AG2 uptake than the untreated one (Figure 4A and B). A similar result was observed from the normal- and cancer-tissue slices obtained immediately after colonoscopic biopsy, which indicates that incubation of the tissue slices in ACSF for 4 h did not significantly influence the relative uptake rate (Figure S8B in the Supporting Information). Furthermore, the uptake could be monitored for more than 3000 s without noticeable decay. These results strongly support the applicability of AG2 in deep-tissue imaging for the diagnosis of colon cancer, in addition to its useful properties for in vivo imaging, namely high photostability and low toxicity.

Colon cancer is known to originate from the mucosa in the intestinal glands and spread into the interior of the tissue,[24] so we have obtained TPM images at different depths from the tissue surface. The TPEF intensities appear scattered at shallow depths due to different degrees of dye adsorption at tissue surfaces that are very different, as shown in the bright-field images (Figure 4A and Figure S8A in the Supporting Information). However, we were able to obtain reliable results at a depth of ≥ 75 μm from the tissue surface. TPM images of the tissue sections obtained for 4000 s revealed the AG2 distribution at depths of 75, 100, 125, and 150 μm, and each image exclusively represents the distribution in a given plane (Figure S8D and S9 in the Supporting Information).

TPM images were obtained up to a depth of 150 μm due to the limited penetration of AG2 into the tissues during the incubation; TPM images at deeper depths could be obtained if the tissues were incubated for a longer period of time. As expected, the uptake was most efficient near the tissue surface; it decreased with larger imaging depths and was negligible at a depth of > 150 μm. In addition, the uptake rate was much slower than that in the cells, probably because of the extracellular matrix, which is more abundant in aged tissues. The sum of the TPEF intensities measured at depths ranging from 75 to 150 μm was largest in the case of cancer tissue, followed by cancer tissue treated with taxol, and then normal tissue (Figure 4C). This result once again clearly demonstrates the preferential uptake of AG2 by cancer tissue and emphasizes the usefulness of AG2 in the diagnosis of colon cancer.

Finally, it is worthwhile to compare the near-infrared (NIR) imaging with the IR dye 800CW-2DG[8] and the TPM imaging with AG2. Both methods are capable of imaging

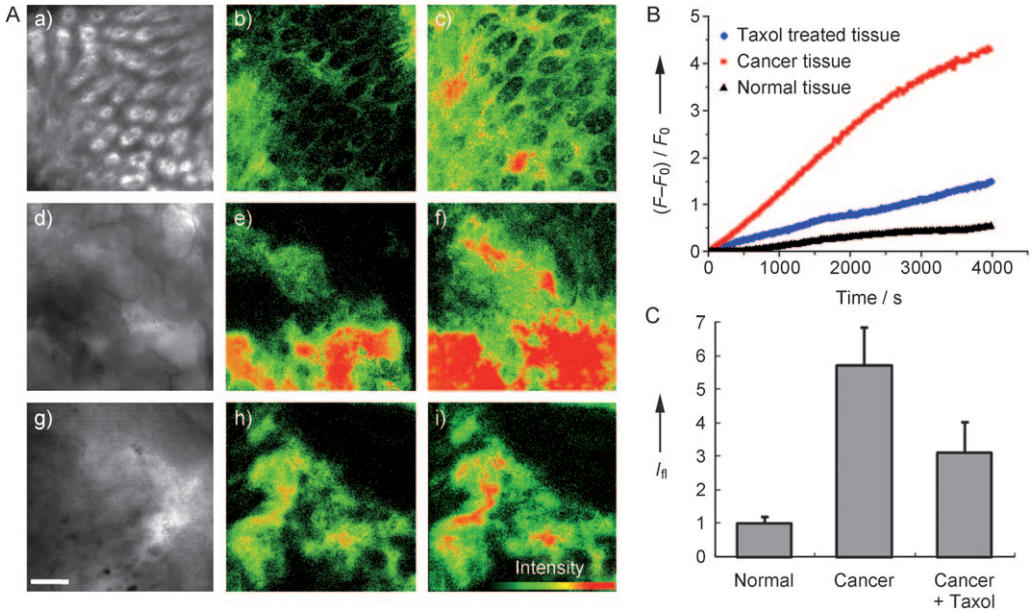

Figure 4. A) Images of normal tissue (a–c), cancer tissue (d–f), and cancer tissue treated with taxol (g–i). Normal tissues were incubated in ACSF for 4 h, and cancer tissues were incubated in the absence and presence of taxol (50 μM) in ACSF for 4 h, after which AG2 uptake was monitored. a, d, and g are bright-field images; b, e, and h are pseudocolored TPM images obtained after incubation with AG2 for 4000 s; and c, f, and i are pseudocolored TPM images obtained after incubation with AG2 for 4 h. The TPM images were obtained at a depth of 100 μm by collecting the TPEF spectra in the range of 520–620 nm on excitation with fs pulses at 780 nm. Scale bar: 30 μm. B) Time course of AG2 uptake by normal tissue, cancer tissue, and cancer tissue treated with taxol (50 μM) at 100 μm depth as a function of time. C) Relative AG2 uptake by normal tissue, cancer tissue, and cancer tissue treated with taxol (50 μM) for 4000 s. The columns indicate the sum of the TPEF intensities measured by photomultiplier tube at depths of 75, 100, 125, and 150 μm from the tissue surface, relative to that of normal tissue. The data are the average of three independent experiments.

deep inside live tissues because of the long excitation wavelengths ($\approx$800 nm). However, the two methods are entirely different. Whereas the former is useful for imaging big objects such as a whole mouse, the latter is suitable for imaging microlevel objects such as cells and tissue slices with high resolution. Due to the localized excitation inherent in the two-photon process and the capability of imaging the pixels (focal point of the laser), TPM images can be obtained at different depths with a few hundred nm resolution (Figure S8 and S9 in the Supporting Information). This is not possible with NIR imaging.

To conclude, we have developed a new TP tracer, AG2, that can be excited by 780 nm fs laser pulses and can be easily taken up by cancer cells and tissues through glucose-specific translocation. AG2 is pH independent at a wide range of physiological pH values (pH 4.0–10) and shows negligible cytotoxicity and high photostability. It can monitor glucose uptake in normal and colon-cancer tissues from human patients for more than 3000 s and can visualize the efficacy of anticancer agents in cancer cells and colon-cancer tissues at depth of 75–150 mm by TPM. This compound may be useful in diagonizing the early stages of cancer and in the development of customized cancer therapy for a patient by comparing the uptake rates of AG2 in normal and cancerous tissues treated with different anticancer drugs at different depths.

Received: March 3, 2009
Revised: August 4, 2009
Published online: September 18, 2009

Keywords: antitumor agents · fluorescent probes · glucose · imaging agents · two-photon microscopy

[1] M. Zhang, Z. Zhang, D. Blessington, H. Li, T. M. Busch, V. Madrak, J. Miles, B. Chance, J. D. Glickson, G. Zheng, *Bioconjugate Chem.* **2003**, *14*, 709.
[2] P. Som, H. L. Atkins, D. Bandoypadhyay, J. S. Fowler, R. R. MacGregor, K. Matsui, Z. H. Oster, D. F. Sacker, C. Y. Shiue, H. Turner, C. N. Wan, A. P. Wolf, S. V. Zabinski, *J. Nucl. Med.* **1980**, *21*, 670.
[3] P. S. Conti, D. L. Lilien, K. Hawley, J. Keppler, S. T. Grafton, J. R. Bading, *Nucl. Med. Biol.* **1996**, *23*, 717.
[4] J. Czernin, M. E. Phelps, *Annu. Rev. Med.* **2002**, *53*, 89.
[5] K. Yoshioka, M. Saito, K. B. Oh, Y. Nemoto, H. Matsuoka, M. Natsume, H. Abe, *Biosci. Biotechnol. Biochem.* **1996**, *60*, 1899.
[6] K. Yoshioka, H. Takahashi, T. Homma, M. Saito, K. B. Oh, Y. Nemoto, H. Matsuoka, *Biochim. Biophys. Acta Gen. Subj.* **1996**, *1289*, 5.
[7] A. Natarajan, F. Srienc, *J. Microbiol. Methods* **2000**, *42*, 87.
[8] J. L. Kovar, W. Volcheck, E. Sevick-Muraca, M. A. Simpson, D. M. Olve, *Anal. Biochem.* **2009**, *384*, 254.
[9] J. Park, H. Y. Lee, M. H. Cho, S. B. Park, *Angew. Chem.* **2007**, *119*, 2064; *Angew. Chem. Int. Ed.* **2007**, *46*, 2018.
[10] D. Thomas, S. C. Tovey, T. J. Collins, M. D. Bootman, M. J. Berridge, P. Lipp, *Cell Calcium* **2000**, *28*, 213.
[11] R. Rudolf, M. Mongillo, R. Rizzuto, T. Pozzan, *Nat. Rev. Mol. Cell Biol.* **2003**, *4*, 579.
[12] W. R. Zipfel, R. M. Williams, W. W. Webb, *Nat. Biotechnol.* **2003**, *21*, 1369.
[13] F. Helmchen, W. Denk, *Nat. Methods* **2005**, *2*, 932.
[14] R. M. Williams, W. R. Zipfel, W. W. Webb, *Curr. Opin. Chem. Biol.* **2001**, *5*, 603.
[15] H. M. Kim, B. H. Jeong, J. Y. Hyon, M. J. An, M. S. Seo, J. H. Hong, K. J. Lee, C. H. Kim, T. Joo, S. C. Hong, B. R. Cho, *J. Am. Chem. Soc.* **2008**, *130*, 4246.
[16] H. M. Kim, C. Jung, B. R. Kim, S. Y. Jung, J. H. Hong, Y. G. Ko, K. J. Lee, B. R. Cho, *Angew. Chem.* **2007**, *119*, 3530; *Angew. Chem. Int. Ed.* **2007**, *46*, 3460.
[17] H. M. Kim, B. R. Kim, J. H. Hong, J. S. Park, K. J. Lee, B. R. Cho, *Angew. Chem.* **2007**, *119*, 7589; *Angew. Chem. Int. Ed.* **2007**, *46*, 7445.
[18] H. M. Kim, M. S. Seo, M. J. An, J. H. Hong, Y. S. Tian, J. H. Choi, O. Kwon, K. J. Lee, B. R. Cho, *Angew. Chem.* **2008**, *120*, 5245; *Angew. Chem. Int. Ed.* **2008**, *47*, 5167.
[19] H. M. Kim, M. J. An, J. H. Hong, B. H. Jeong, O. Kwon, J. Y. Hyon, S. C. Hong, K. J. Lee, B. R. Cho, *Angew. Chem.* **2008**, *120*, 2263; *Angew. Chem. Int. Ed.* **2008**, *47*, 2231.
[20] C. Xu, W. W. Webb, *J. Opt. Soc. Am. B* **1996**, *13*, 481.
[21] M. Murata, M. Akao, B. O'Rourke, E. Marban, *Circ. Res.* **2001**, *89*, 891.
[22] K. Yamada, M. Nakata, N. Horimoto, M. Saito, H. Matsuoka, N. Inagaki, *J. Biol. Chem.* **2000**, *275*, 22278.
[23] R. G. O'Neil, L. Wu, N. Mullani, *Mol. Imaging Biol.* **2005**, *7*, 388.
[24] L. D. Zinkin, *Dis. Colon Rectum* **1983**, *26*, 37.
[25] *The Handbooks—A Guide to Fluorescent Probes and Labeling Techonologies* (Ed.: R. P. Haugland), 10th ed., Molecular Probes, Eugene, OR, **2005**.

